Uncertainty in Predicted Tropical Cyclone Path and Landfall Characteristics for Landfalling Storms to Support External Hazard Probabilistic Risk Assessments for Critical Infrastructure – A Preliminary Analysis

Somayeh Mohammadi[a], Michelle Bensi[b], Zhegang Ma[c], and Kaveh Faraji Najarkolaie[d]

[a] University of Maryland, College Park, USA, somayeh@terpmail.umd.edu

[b] University of Maryland, College Park, USA, mbensi@umd.edu

[c] Idaho National Laboratory, USA, zhegang.ma@inl.gov

[d] University of Maryland, College Park, USA, kfaraji@terpmail.umd.edu

Abstract: Critical infrastructure facilities, such as nuclear power plants, are often located in coastal regions exposed to tropical cyclones (TCs). These facilities may employ permanent protective measures as well as strategies that require manual (human) actions to install temporary features (e.g., flood protection berms and pumps). In addition to the possibility of hardware failures, there is a possibility that actions will be unsuccessful due to delayed organizational decision-making, human errors, and differences between predicted and experienced hazard characteristics. Accurate external hazard probabilistic risk assessments (XHPRAs) must quantify these error probabilities, which depend on factors such as the information available to support decisions, the time available to perform actions, and the environmental conditions under which actions are performed. These factors are subject to uncertainty due to uncertainty in TC forecasts. To support XHPRAs for critical infrastructure facilities, this paper seeks to explore uncertainty in the conditions under which human actions will be performed, with particular emphasis on the time available to execute actions. We analyzed National Oceanic and Atmospheric Administration (NOAA) geographic information system (GIS) datasets related to advisory forecast TC track data for 2012-2020. For each historic storm, we compared advisory forecasted track data (e.g., predicted landfall locations, times, and wind speed) to the observed track to understand errors and uncertainty.

1. INTRODUCTION

When tropical cyclones (TCs) are predicted to make landfall, critical infrastructure facilities such as nuclear power plants (NPPs) must make decisions about the implementation of protective measures and changes to their operating status. For example, in response to a forecast, a facility may decide to shut down, take protective actions, or continue normal operations. These decisions are often based on forecasts of when the storm will make landfall, the landfall location, and the storm's severity (e.g., estimated wind speed or storm surge). However, if the forecast is inaccurate or if the forecast uncertainty is not communicated effectively to decision-makers, there may be consequences for facilities not prepared for the storm. Conversely, a facility may shut down unnecessarily, leading to a loss of ability to provide infrastructure services.

External hazard probabilistic risk assessments (XHPRAs) are used to systematically assess the risks posed by external hazards such as TCs. XHPRAs often consider human reliability analysis (HRA) in assessing the reliability of protective or mitigating strategies. Such assessments require estimates of the uncertainty associated with the time available to implement actions (which depends on the estimated time and location of landfall of a TC) and the conditions under which actions will be performed. However, to date, there have not been systematic assessments of uncertainties associated with TC forecasts in a manner amenable to characterizing uncertainties required for an XHPRA.

This study aims to analyze the uncertainty in TC landfall timing, location, and severity with the specific goal of presenting information in a manner amenable to inclusion in the XHPRAs for critical

infrastructure facilities such as NPPs. Particular emphasis is placed on understanding the difference between the assumed time available (based on procedures) and the actual time until the onset of adverse storm conditions. This paper describes an in-progress analysis being performed for historical storms affecting the Atlantic and Pacific coasts of North and Central America. Preliminary results are presented, and the next steps are outlined. This work is part of a larger effort described in a companion paper presented at this conference [1].

2. EXISTING RESOURCES AND CONTEXT

For storms in the Atlantic and Northeast and North Central Pacific basins, the United States National Oceanic and Atmospheric Administration (NOAA), National Hurricane Center (NHC) issues information related to the forecasted position of a storm (storm track centerline) and maximum 1-min surface wind speeds. NHC forecasts are typically released every six hours (at 0300, 0900, 1500, and 2100 UTC). The prediction periods related to these forecasts are 12, 24, 36, 48, 72, 96, and 120 hours after the forecast's nominal time [2].

NOAA NHC periodically releases NHC Forecast Verification Reports [3] that compare forecasts for a TC with the estimated "best track" for the TC. The TC best track is estimated after the event as part of a post-storm analysis, which may include observational data that was not available in real-time and other post-storm analyses [4], [5]. In the verification reports [3], track forecast error is defined as the maximum (great circle) distance between the forecast position of the cyclone and the best track position at the time of the forecast. The error in the forecasted intensity of the storm is also defined as the absolute difference between the forecasted intensity and the best track intensity at the forecast time. NOAA has estimated these errors as annual mean errors and five-year mean errors. Trends over time are also analyzed. NOAA's verification reports aim to help answer inquiries about the accuracy and skill of forecasts and computer models. NOAA’s verification reports are focused on overall accuracy over various forecast durations, but do not assess performance, in predicting the time and location of landfall, which is particularly relevant in the context of XHPRAs.

In addition to predictions related to the position of a storm center track, NHC forecasts also include a "cone of uncertainty" reflecting uncertainty in the forecasted storm track centreline. Based on the definition provided by NOAA, the cone of uncertainty represents the probable track of the storm. This cone is formed by enclosing the area swept out by several circles along the forecast track. The size of each circle is set to cover two-thirds of historical official forecast errors for a five-year sample. However, the problem is that people often misinterpret the cone of uncertainty [6]. Under this misinterpretation, people assume there is a high chance of being in the path of a hurricane for those who live inside the cone while those outside the cone are safe from potential hurricane effects. Furthermore, it is difficult for people to distinguish the cone as a region experiencing the storm effects from a region that the storm path will pass [7]. Therefore, some studies focused on time-specific visualization of the predicted storm track and its uncertainty. [7], [8].

This study focuses on analyzing the uncertainty related to forecasted landfall characteristics of the storm. These characteristics include landfall location, time, and wind speed. This work is interested in analyzing the error related to characteristics of landfall predictions and how the forecast values are different from observations. Several existing studies have estimated forecast error of NHC forecasts related to storm track position and wind speed. However, these studies were not focused on analyzing the forecast errors related to landfall characteristics of the storm. For example, Rappaport et al [9] analyzed the forecast error of storm track. This work was focused on estimating the error related to predicted storm track position and intensity and has used best track data. Track forecast error was estimated as the great circle distance between the center of forecasted TCs and the best track position at the time of the forecast. Error related to storm intensity was estimated as the absolute difference between forecast and best track value at the time of forecast verification. This study estimated mean forecast errors in four different periods of data including 1970-1979, 1980-1989, 1990-1999, and 2000-2008. The results of this study showed how forecast values improved in recent years. For example, forecast error for 48-hr forecast wind speed decreased from 250 nautical mile (nm) in 1970-1979 to 100

nm in 2000-2008. Furthermore, a study by Franklin, et al [10] showed that 24, 48, and 72-hr forecasts were improved at an annual rate of 1.3, 1.9, and 2% (respectively) for the period of 1970-2001. In the study by Zhang, et al [11], the errors of lead forecast times provided by NHC official forecasts were computed for the purposes of comparing against a hurricane prediction system that used a Kalman filter method for assimilating high-resolution radar observations. Using this method, mean absolute errors for intensity forecasts related to 24 to 120-hr lead forecast times were 20 to 40% lower compared to NHC official forecasts at similar times.

While this study focuses on informing uncertainty characterizations for XHPRA for critical infrastructure, the uncertainty in forecasted location and lead time (i.e., the length of time between the issuance of a forecast and the time at which the storm affects a location) also affects evacuation decisions. For example, Lindell and Prater [12] modeled how uncertainties in the prediction of hurricane behavior affect an evacuation management decision support system. The study provided information regarding the "minimum, most, and maximum probable evacuation time estimate" versus the "earliest, most, and latest probable estimated times of arrival" for the storm. Lindell and Prater (2007) also estimated the cost of decision errors related to an unnecessary evacuation (false positive) and a late evacuation (false negative). A study by Regnier [13] investigated the relationship between lead time and storm track uncertainty for Atlantic hurricanes. They explored "threats" versus "strikes" as a function of lead time for several cities.

Beyond evacuation modeling, studies have also looked at track uncertainty from the perspective of modeling hazard impacts (e.g., storm surge) [14], [15]. A recent study by Kang (2020) used a Bayesian approach for updating the uncertainty of operational track forecast errors.

3. DATA AND METHODS

The NHC issues advisories [17] for TCs that develop in the Atlantic and Eastern Pacific basins. The products are issued at least every 6 hours, typically at pre-set times. Advisories contain information about (1) current coastal watches/warnings, (2) the TC's current storm center location and maximum sustained winds, (3) the predicted track of the storm (location and wind speed), and (4) a cone of uncertainty. The cone uncertainty provides uncertainty related to the centerline of the storm, not the spatial extent of the storm [17].

Archived geographic information system (GIS) storm advisory data (as zipped Keyhole Markup Language [KMZ] files) from the NHC [2] was collected for the analysis herein. Figure 1 shows the structure of data as formatted for use in this study. Each downloaded advisory is associated with one set of "observational values," which includes the location (storm center), wind speed, and the minimum pressure of a storm when each storm advisory is issued. For example, Figure 2a shows the estimated location and wind speed of Hurricane Debby (2012) at the times that advisories were issued. In addition, the advisory data includes the forecasted location and windspeed of storms for 12, 24, 36, 48, 72, and 96-hour predictions. Figure 2b shows the location of Hurricane Debby (2012) at the time one example advisory was issued along with the 12, 24, 36, 48, 72, and 96-hour predicted locations. Figure 2c shows the forecasted tracks of Hurricane Debby (2012) associated with each advisory. It is noted that there is a 3-hour time lag between the initiation and eventual issuance of a forecast. Therefore, the forecast times (i.e., 12, 24, 36, 48, 72, and 96-hours) correspond to the time between the nomimal initial time for a forecast (i.e., the time at which the forecast process is initiated) at the time associated with a forecast. For example, there will typically be a 9-hour (12 hours minus 3 hours) difference between the forecast issuance time and the time associated with the 12-hour prediction.

Figure 1. Structure of data used in uncertainty analysis

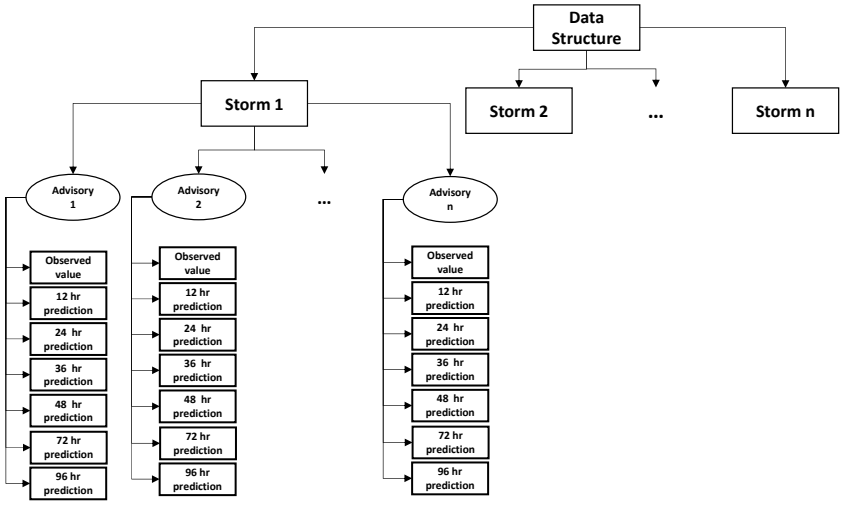

GIS data related to 347 TC track data for the years 2012 to 2020 for both the Atlantic and Eastern Pacific basins was collected. Future work will seek to expand the time period included in the analysis. Data was processed into the format shown in Figure 1 by extracting latitude, longitude, time, and wind speed data related to observed and predicted values. For this study, the advisory data corresponding to the documented location and windspeed of storms when the advisories are issued are treated as the "observed track" for the storm. This location and windspeed data values may differ from the "best tracks" later calculated as part of the NHC Hurricane Database HURDAT re-analysis efforts [18]. For example, Figure 2d shows the Hurricane Debby (2012) "observed track" (as constructed using advisory location/windspeed data) and the HURDAT best track. Future work will explore the potential impact of replacing the advisory "observational values" with the HURDAT best track values.

Figure 2. (a) Estimated location and wind speed of Hurricane Debby (2012) at the times that advisories were issued; (b) Location of Hurricane Debby (2012) at the time one example advisory (red circle)was issued along with the 12, 24, 36, 48, 72, and 96-hour predicted locations (black circles); (c) Predicted tracks (dashed lined) of Hurricane Debby (2012) associated with each advisory (location of storm at time advisory issues shown by black stars); (d) Hurricane Debby (2012) track as constructed using advisory location/windspeed data (dashed lines with circles) and based on HURDAT best track (solid lines with circles)

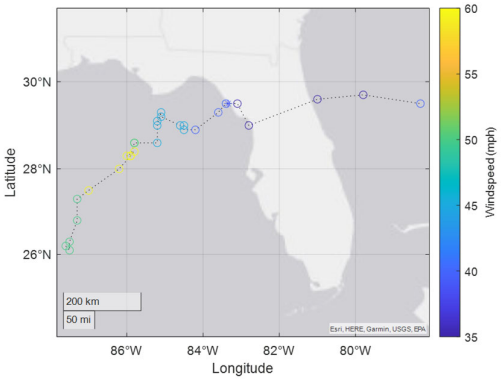

(a)

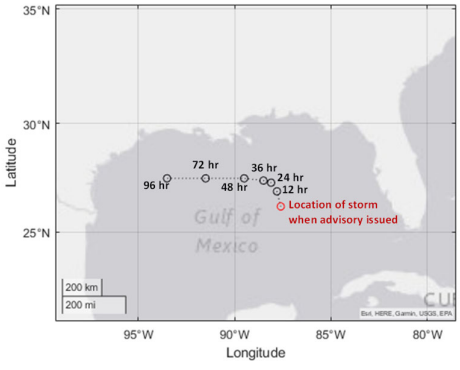

(b)

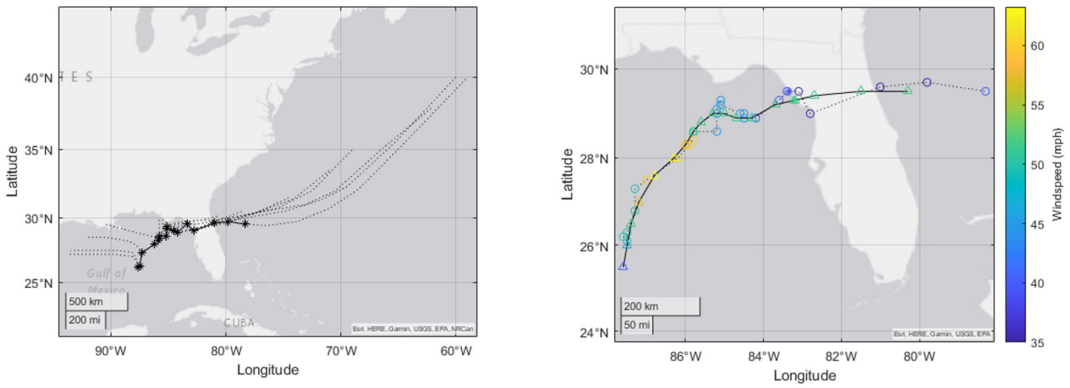

(c) (d)

The landfall locations of each observed and predicted track are estimated by intersecting the storm track with an idealized version of the coastline of North America. Then windspeed values at landfall and the time of landfall are linearly interpolated based on the distance traveled between available latitude/longitude points. Figure 3 shows all observed tracks (as computed using the location of storm centers when advisories are issued) for historical storms from 2012 to 2020 originating in the Atlantic and Pacific basins, along with the interpolated landfall locations for the storms that made landfall. Ultimately, 87 landfalling storms (i.e., storms for which the observed track intersected with the idealized coastline) were considered in the analysis that follows. Of the 87 storms, 84 of the storms included at least one advisory track predicting landfall (i.e., the predicted track intersected the idealized coastline).

Figure 3. Observational points for all historical storms (black lines) for 2012-2021, along with origin locations (red dots), and interpolated landfall locations (cyan circles) for (a) Atlantic Basin-originating storms and (b) Pacific basin-originating storms

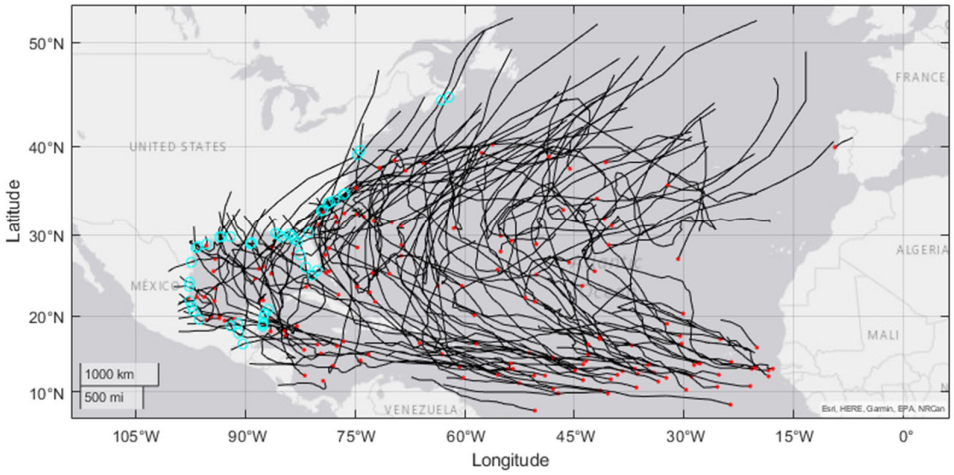

(a)

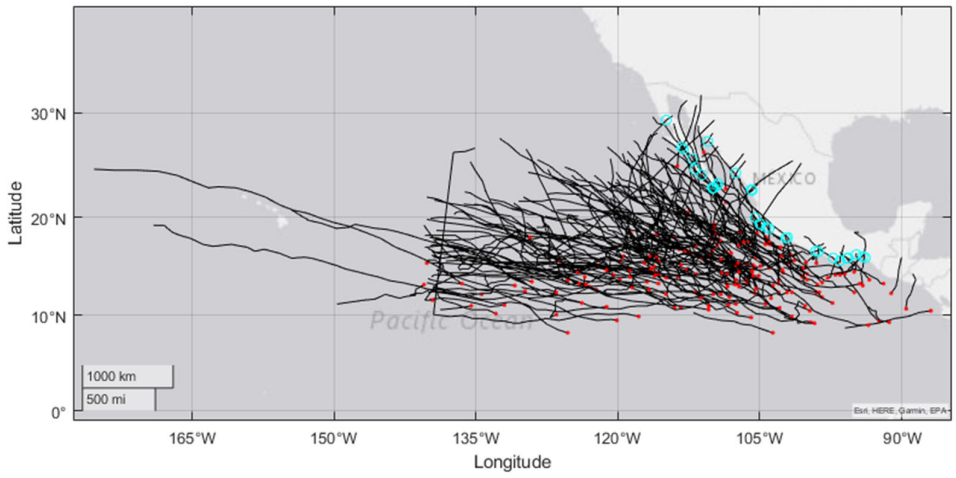

(b)

For each landfalling storm i and each associated storm advisory j, the observed and predicted track data was used to compute the following quantities:

- $t_{i,j}^{[a]}$ =the time elapsed between the issuance of advisory j for storm i and the interpolated observed landfall time of storm i (hours)
- $t_{i,j}^{[p]}$ =the time elapsed between the issuance of advisory j for storm i and the interpolated time of landfall (based on the predicted storm track) for storm i and advisory j (hours)
- $w_i^{[a]}$ = interpolated observed wind speed at landfall for storm i (mph)
- $w_{i,j}^{[p]}$ = interpolated predicted wind speed at landfall from advisory j for storm i (mph)
- $d_{i,j}$ = distance between the interpolated observed landfall location of storm i and the interpolated predicted landfall location of storm i from advisory j for storm i (miles)

Using the above quantities, the following error metrics are also calculated:

- Time to landfall prediction error: $\varepsilon_{ij}^{[t]} = t_{i,j}^{[p]} - t_{i,j}^{[a]}$
- Landfall wind speed prediction error: $\varepsilon_{ij}^{[w]} = w_{i,j}^{[p]} - w_i^{[a]}$

4. ANALYSIS RESULTS

Across the 84 predicted landfalling storms in the dataset, there are 717 pairwise observations in which both values of $t_{i,j}^{[a]}$ and $t_{i,j}^{[p]}$ are available for a particular 12, 24, 36, 48, 72 or 96-hr advisory. These pairwise combinations of the observed and predicted landfall time are shown in the scatterplot in Figure 4a, with colors indicating the distance between the observed and predicted interpolated landfall locations. The majority of points are clustered around the 45° line. However, in selected cases, large differences between $t_{i,j}^{[a]}$ and $t_{i,j}^{[p]}$ are identified, indicating that the time to landfall is substantially larger than predicted. This is primarily caused by differences in the observed and predicted location of landfall, as can be observed by the larger distances associated with data pairs located farther from the reference line in Figure 4a. For example, considering the storm track and predictions shown in Figure 5a. Initially, landfall was predicted to occur in Florida, but landfall ultimately occurred much later and much farther north. Figure 4b presents a histogram of the associated percent errors values $\left(100 * \frac{\varepsilon_{ij}^{[t]}}{t_{i,j}^{[a]}}\right)$, considering only observations for which $d_{i,j} \leq 500$ miles. The majority (59%) of computed values of $\varepsilon_{ij}^{[t]}$ are

positive, indicating that the actual time to landfall was shorter than predicted. Approximately 40% of data pairs are associated with a percent error of $\pm$ 10%.

There are likewise 717 data pairs for which values of $w_i^{[a]}$ and $w_{i,j}^{[p]}$ are available. The scatterplot of $w_i^{[a]}$ and $w_{i,j}^{[p]}$ and histogram of percent error $\left(100 * \frac{\varepsilon_{ij}^{[w]}}{w_{i,j}^{[a]}}\right)$ are shown in Figure 4c and Figure 4d, respectively. Negative values of $\varepsilon_{ij}^{[w]}$ indicate observed windspeeds landfall exceed those that are predicted. Negative values were encountered for about half of the available data pairs.

Figure 4. (a) Scatterplot of $t_{i,j}^{[a]}$ and $t_{i,j}^{[p]}$; (b) Histogram of percent error $\left(100 * \frac{\varepsilon_{ij}^{[t]}}{t_{i,j}^{[a]}}\right)$ (a) Scatterplot of $w_i^{[a]}$ and $w_{i,j}^{[p]}$; (b) Histogram of percent error $\left(100 * \frac{\varepsilon_{ij}^{[w]}}{w_{i,j}^{[a]}}\right)$

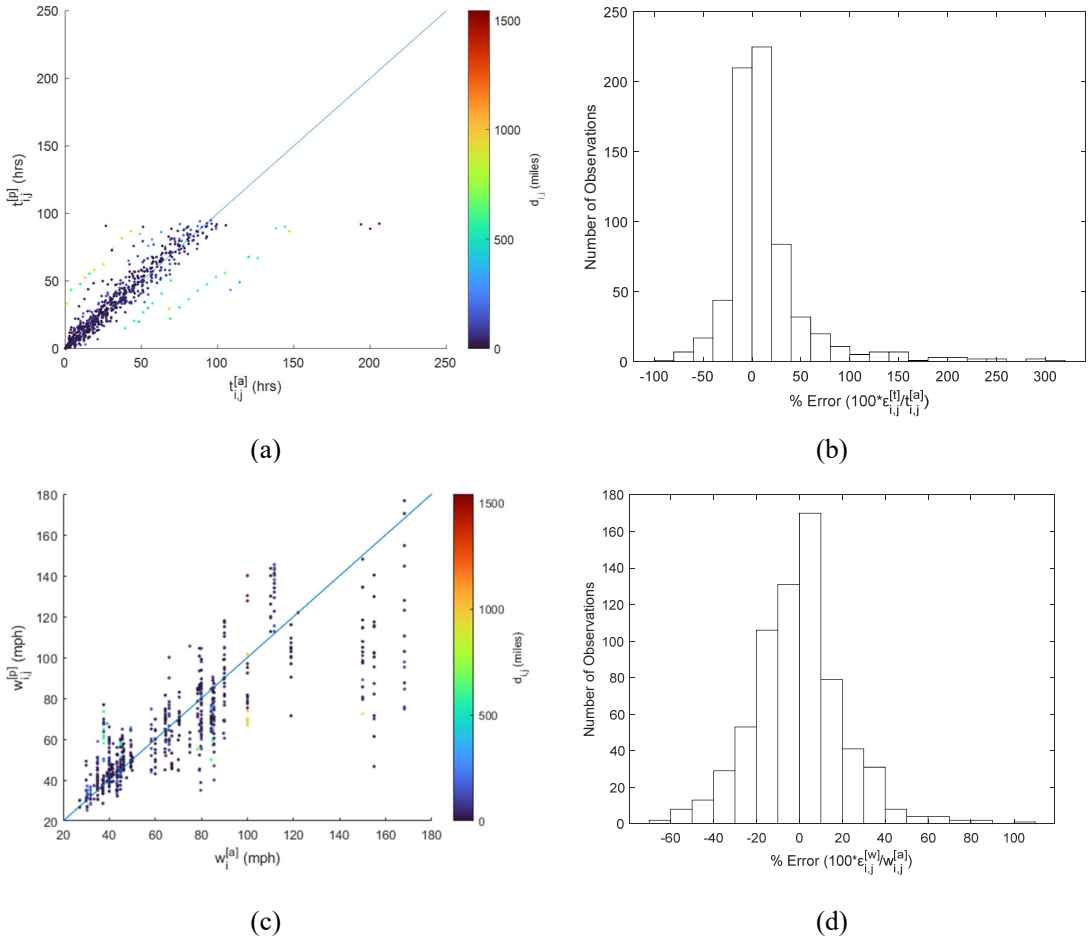

Figure 5b shows a scatter plot of computed percent error values for wind and timing (considering $d_{i,i} \leq$ 500 miles), with colors indicated by $d_{i,j}$. Annotations are provided showing the percentage of pairwise observations falling into each quadrant. In general, errors are clustered around (0,0), with asymmetry noted in the errors in landfall times, which are more likely to take on larger values.

Figure 5. (a) Example hurricane track with a large negative value of $\varepsilon_{ij}^{[t]}$; (b) Scatterplot computed percent error values (considering $d_{i,i} \leq 500$ miles) with colors indicated by $d_{i,j}$ (annotations show the percentage of pairwise observations falling into each quadrant).

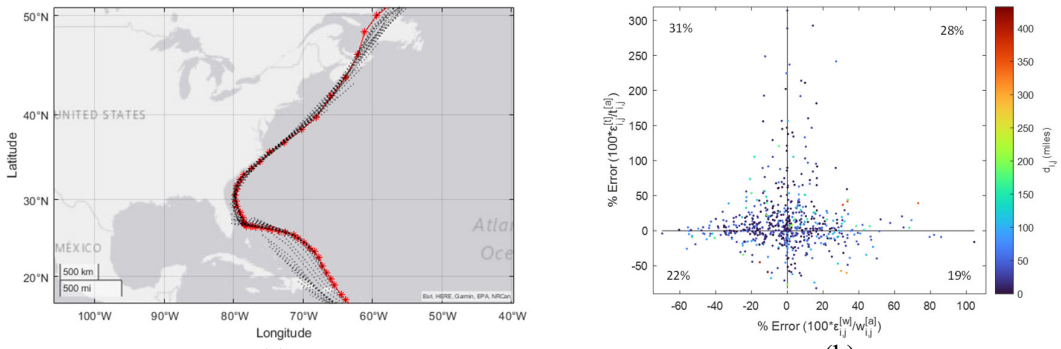

(a) (b)

The above results present analysis metrics across all pairwise combinations, including advisories for 12 through 96 hours after the nominal initial forecast time. In the context of XHPRA, it is also of interest to understand the uncertainty in the time available to execute procedures, considering the information that will typically be used as the basis for initiation of protection or mitigation measures. For example, a procedure may require the implementation of protective actions (e.g., to install flood protection measures or pre-stage mitigation equipment) when a hurricane is predicted to make landfall in a region within the next 24 hours.

To understand how uncertainty may change with the assumed "action trigger times" (i.e., the time when actions are initiated based on the predicted time until storm landfall), the quantity $t_{i,j}^{[p]}$ is used to partition the dataset. Specifically, four different action trigger times are considered: $t_{trig} = 12$, 24, 36, and 48 hours. For each storm $i = 1, \ldots, 84$, the first advisory j for which $t_{i,j}^{[p]} \leq t_{trig}$ is identified, and the associated values of $t_{i,j}^{[a]}$ and $t_{i,j}^{[p]}$ are extracted. The corresponding scatterplots of $t_{i,j}^{[a]}$ and $t_{i,j}^{[p]}$ (with colors representing interpolated observed wind speed at landfall) are shown in Figure 6. The percent of observations for which $t_{i,j}^{[a]} \leq t_{i,j}^{[p]}$ (i.e., actual time until landfall is less than the predicted time) and the correlation coefficient between $t_{i,j}^{[a]}$ and $t_{i,j}^{[p]}$ are shown in Table 1. In general, the percent of observations (53-60%) for which the actual time to landfall is less than predicted time is fairly constant across the four sets of information.

It is noteworthy that there are instances in which both the actual and predicted time to landfall are substantially shorter than the assumed trigger time. This was observed to be the result of several situations, some of which are related to the actual evolution of the TC event and others that are artifacts of the analysis that has been performed. For example, time to landfall values that are substantially shorter than t_{trig} can be caused by situations in which the first advisory was issued relatively close to the time of landfall (e.g., see Figure 7a), by changes in the track such that landfall is not predicted until relatively close to the observed landfall (e.g., see Figure 7b), or by situations in which the distinction between a landfalling and bypassing track is relatively minor (e.g., see Figure 7c). Some of these issues may be addressed by analyzes that extend beyond a centreline analysis.

Figure 6. Scatterplot of $t_{i,j}^{[a]}$ and $t_{i,j}^{[p]}$ considering a trigger time of (a) 12 hrs, (b) 24 hrs, (c) 36 hrs, (d) 48 hrs

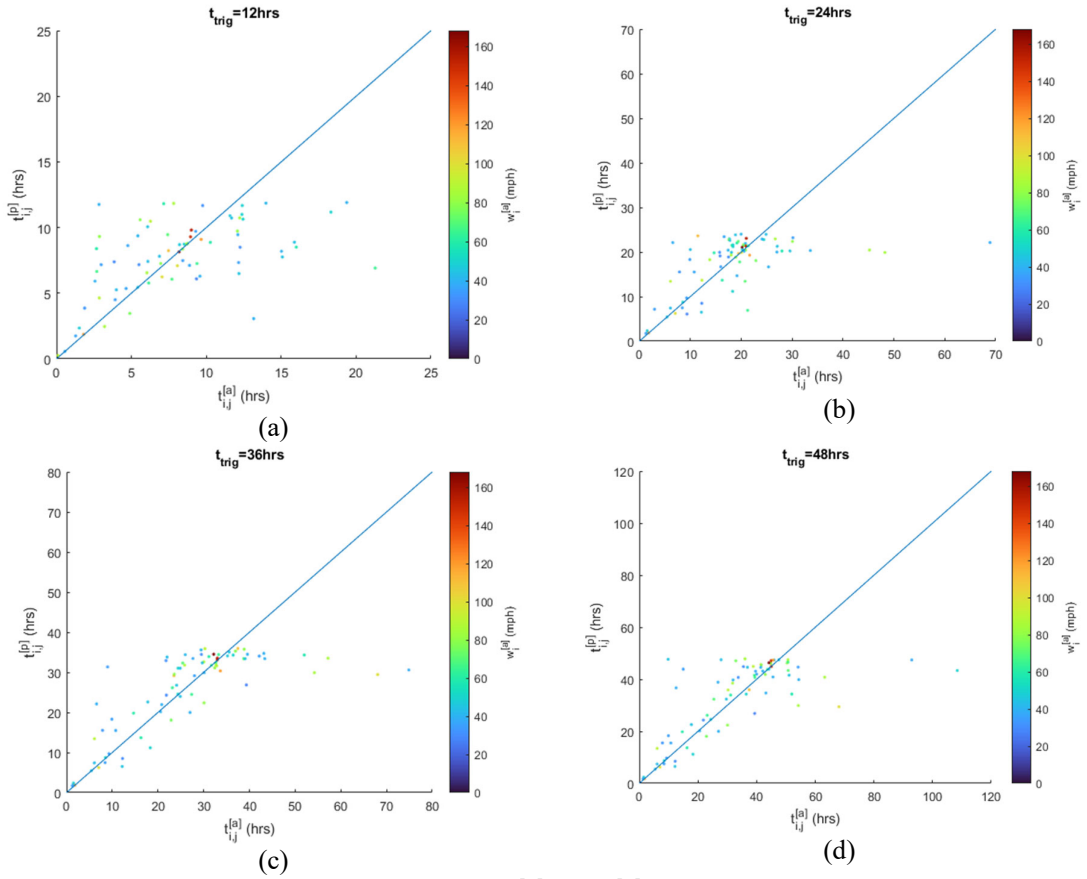

Table 1. Basic statistics regarding $t_{i,j}^{[a]}$ and $t_{i,j}^{[p]}$ for multiple action trigger times

t_{trig}	% of observations with $t_{i,j}^{[a]} \leq t_{i,j}^{[p]}$	Correlation between $t_{i,j}^{[a]}$ and $t_{i,j}^{[p]}$	# of observed landfalls
12-hr	53%	0.53	77
24-hr	57%	0.55	80
36-hr	53%	0.73	80
48-hr	60%	0.71	82

Figure 7. Examples of tracks for which $t_{i,j}^{[a]}$ and $t_{i,j}^{[p]}$ are substantially shorter than t_{trig} (red lines show observed track, dashed black lines show predicted tracks, and the yellow star indicates the interpolated observed landfall location)

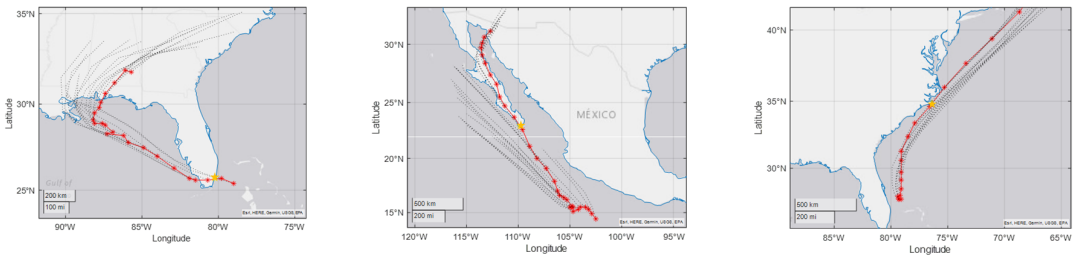

5. NEXT STEPS

Several areas for future work and analysis refinements have been noted throughout the text. These issues will be addressed as part of future research activities. In addition, it is noted that this preliminary study analyzed storm track uncertainty in timing location and wind speed, considering only the centreline for the storm. This study did not consider the entire radial extent of the storm. For example, Figure 8a shows the observed wind radii (i.e., the maximum extent of sustained winds for several wind speed thresholds), and Figure 8b shows an example of predicted wind radii. Future work will consider information related to wind radii to capture better the spatial extent of the storm and its impacts. This is expected to yield substantially more relevant insights than an analysis focusing exclusively on the centerline of the storm. Future work will also consider insights derived through analyzes involving the cone of uncertainty (Figure 8c). Further, the current analysis does not differentiate between hurricanes in the Atlantic and Eastern Pacific basins. It also does not explore the relationship between errors of prediction as a function of hurricane parameters. Future work is expected to explore these issues. Longer term, future work may consider alternate hurricane prediction models and other hazards.

Figure 8. (a) Observed wind radii of Hurricane/Storm Sandy (2012) (the storm track is shown by the red centerline and the red, pink, and grey shapes show wind radii); (b) Example of 72-hour predicted wind radii for Hurricane/Storm Sandy (2012) (the storm track is shown by the red centerline and the pink and grey shapes show wind radii); (c) Example cone of uncertainty (the storm track is shown by the red centerline and the cone of uncertainty is shown in grey)

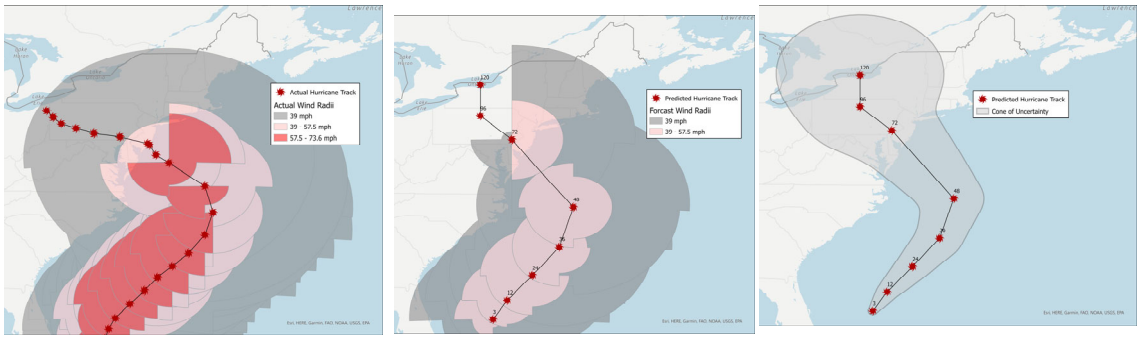

(a) (b) (c)

6. CONCLUSION

When a storm is predicted to make landfall, critical facilities such as NPPs will typically take protective actions before the storm makes landfall. XHPRAs often consider HRA in assessing the reliability of protective or mitigating strategies. Such assessments require estimates of the uncertainty associated with the time available to implement actions (which depends on the estimated time and location of landfall of a TC) and the conditions under which actions will be performed. This study seeks to understand and characterize uncertainty in the time available to perform actions by exploring how the time/location/wind speed at landfall differs from values predicted as part of NOAA advisories. This preliminary study considers geospatial analysis using observed and predicted storm track centerlines. Preliminary results indicate that there is a tendency for actual times to landfall to be shorter than predicted, indicating that the actual time available to implement procedural actions may be shorter than assumed. In general, a shorter time available to complete actions will increase human failure probabilities. Further analysis is required to confirm the results of this initial assessment. Specifically, future work will consider the radial extent of storms to provide a more comprehensive assessment.

Acknowledgements

This research is supported by a research grant from the Department of Energy's Nuclear Energy University Program (NEUP) under grant/cooperative agreement DE-NE0008974. The creation of some figures was supported under a U.S. Nuclear Regulatory Commission Faculty Development Grant [31310018M0043]. Any opinions, findings, and conclusions expressed in

this paper/presentation are those of the authors and do not necessarily reflect the views of the funding agency or any other organization.

References

[1] M. Bensi, S Mohammadi, N. Ghosh, T. Liu, C. Levine, A. Al-Douri, R. Schneider, Z. Wu, K. Groth, Z. Ma, "Identifying and Prioritizing Sources of Uncertainty in External Hazard Probabilistic Risk Assessment: Project Activities and Progress," presented at the PSAM 16, Honolulu, HI, 2022.

[2] NOAA NHC, "NHC Data in GIS Formats," *National Hurricane Center and Central Pacific Hurricane Center*, 2022. https://www.nhc.noaa.gov/gis/ (accessed Feb. 28, 2022).

[3] NOAA NHC, "National Hurricane Center Forecast Verification," *National Hurricane Center and Central Pacific Hurricane Center*, 2017. https://www.nhc.noaa.gov/verification/index.shtml? (accessed Feb. 28, 2022).

[4] C. Landsea, J. Franklin, E. Blake, and R. Tanabe, "Revised Northeast and North Central Pacific hurricane database (HURDAT2)," NOAA, Feb. 2016. [Online]. Available: https://www.nhc.noaa.gov/data/hurdat/hurdat2-format-nencpac.pdf

[5] C. Landsea and J. Beven, "Revised Atlantic hurricane database (HURDAT2)," NOAA, Nov. 2019. [Online]. Available: https://www.nhc.noaa.gov/data/hurdat/hurdat2-format-nov2019.pdf

[6] K. Broad, A. Leiserowitz, J. Weinkle, and M. Steketee, "Misinterpretations of the 'Cone of Uncertainty' in Florida during the 2004 Hurricane Season," *Bulletin of the American Meteorological Society*, vol. 88, no. 5, pp. 651–668, May 2007, doi: 10.1175/BAMS-88-5-651.

[7] J. Cox, D. House, and M. Lindell, "VISUALIZING UNCERTAINTY IN PREDICTED HURRICANE TRACKS," *IJUQ*, vol. 3, no. 2, 2013, doi: 10.1615/Int.J.UncertaintyQuantification.2012003966.

[8] L. Liu, M. Mirzangar, R. M. Kirby, R. Whitaker, and D. H. House, "Visualizing Time-Specific Hurricane Predictions, with Uncertainty, from Storm Path Ensembles," *Comput. Graph. Forum*, vol. 34, no. 3, pp. 371–380, Jun. 2015, doi: 10.1111/cgf.12649.

[9] E. N. Rappaport *et al.*, "Advances and Challenges at the National Hurricane Center," *Weather and Forecasting*, vol. 24, no. 2, pp. 395–419, Apr. 2009, doi: 10.1175/2008WAF2222128.1.

[10] J. L. Franklin, C. J. McAdie, and M. B. Lawrence, "Trends in Track Forecasting for Tropical Cyclones Threatening the United States, 1970–2001," *Bulletin of the American Meteorological Society*, vol. 84, no. 9, pp. 1197–1204, Sep. 2003, doi: 10.1175/BAMS-84-9-1197.

[11] F. Zhang, Y. Weng, J. F. Gamache, and F. D. Marks, "Performance of convection-permitting hurricane initialization and prediction during 2008–2010 with ensemble data assimilation of inner-core airborne Doppler radar observations," *Geophysical Research Letters*, vol. 38, no. 15, 2011, doi: 10.1029/2011GL048469.

[12] M. K. Lindell and C. S. Prater, "A hurricane evacuation management decision support system (EMDSS)," *Nat Hazards*, vol. 40, no. 3, pp. 627–634, Mar. 2007, doi: 10.1007/s11069-006-9013-1.

[13] E. Regnier, "Public Evacuation Decisions and Hurricane Track Uncertainty," *Management Science*, vol. 54, no. 1, pp. 16–28, 2008, Accessed: May 25, 2022. [Online]. Available: https://www.jstor.org/stable/20122357

[14] A. P. Kyprioti, E. Adeli, A. A. Taflanidis, J. J. Westerink, and H. L. Tolman, "Probabilistic Storm Surge Estimation for Landfalling Hurricanes: Advancements in Computational Efficiency Using Quasi-Monte Carlo Techniques," *Journal of Marine Science and Engineering*, vol. 9, no. 12, Art. no. 12, Dec. 2021, doi: 10.3390/jmse9121322.

[15] A. A. Taylor and B. Glahn, "PROBABILISTIC GUIDANCE FOR HURRICANE STORM SURGE," p. 8, Jan. 2008.

[16] N. Kang, "A Bayesian Representation of the Storm Approach Probability Based on Operational Track Forecast Errors," *Weather and Forecasting*, vol. 35, no. 5, pp. 2025–2032, Oct. 2020, doi: 10.1175/WAF-D-20-0040.1.

[17] NOAA, "Hurricane and Tropical Storm Watches, Warnings, Advisories and Outlooks." https://www.weather.gov/safety/hurricane-ww (accessed May 23, 2022).

[18] NOAA, "HURDAT Re-analysis Project (Hurricane Database)," *Hurricane Research Division*, 2021. https://www.aoml.noaa.gov/hrd/hurdat/Data_Storm.html (accessed May 23, 2022).